Title

Calcium channel selectivity for divalent and monovalent cations. Voltage and concentration dependence of single channel current in ventricular heart cells.

Journal

The Journal of general physiology, 88(3)

ISSN

0022-1295

Authors

Hess, P
Lansman, JB
Tsien, RW

Publication Date

1986-09-01

DOI

10.1085/jgp.88.3.293

Peer reviewed

Calcium Channel Selectivity for Divalent and Monovalent Cations

Voltage and Concentration Dependence of Single Channel Current in Ventricular Heart Cells

PETER HESS, JEFFRY B. LANSMAN, and RICHARD W. TSIEN

From the Department of Physiology, Yale University School of Medicine, New Haven, Connecticut 06511

ABSTRACT Single channel and whole cell recordings were used to study ion permeation through Ca channels in isolated ventricular heart cells of guinea pigs. We evaluated the permeability to various divalent and monovalent cations in two ways, by measuring either unitary current amplitude or reversal potential (E_{rev}). According to whole cell measurements of E_{rev}, the relative permeability sequence is $Ca^{2+} > Sr^{2+} > Ba^{2+}$ for divalent ions; Mg^{2+} is not measurably permeant. Monovalent ions follow the sequence $Li^+ > Na^+ > K^+ > Cs^+$, and are much less permeant than the divalents. These whole cell measurements were supported by single channel recordings, which showed clear outward currents through single Ca channels at strong depolarizations, similar values of E_{rev}, and similar inflections in the current-voltage relation near E_{rev}. Information from E_{rev} measurements stands in contrast to estimates of open channel flux or single channel conductance, which give the sequence Na^+ (85 pS) > Li^+ (45 pS) > Ba^{2+} (20 pS) > Ca^{2+} (9 pS) near 0 mV with 110–150 mM charge carrier. Thus, ions with a higher permeability, judged by E_{rev}, have lower ion transfer rates. In another comparison, whole cell Na currents through Ca channels are halved by <2 μM $[Ca]_o$, but >10 mM $[Ca]_o$ is required to produce half-maximal unitary Ca current. All of these observations seem consistent with a recent hypothesis for the mechanism of Ca channel permeation, which proposes that: (*a*) ions pass through the pore in single file, interacting with multiple binding sites along the way; (*b*) selectivity is largely determined by ion affinity to the binding sites rather than by exclusion by a selectivity filter; (*c*) occupancy by only one Ca ion is sufficient to block the pore's high conductance for monovalent ions like Na^+; (*d*) rapid permeation by Ca ions depends upon double occupancy, which only becomes significant at millimolar $[Ca]_o$ because of electrostatic repulsion or some other interaction between ions; and (*e*) once double occupancy

Address reprint requests to Dr. Peter Hess, Dept. of Physiology and Biophysics, Harvard University, 25 Shattuck St., Boston, MA 02115. Dr. Lansman's present address is Dept. of Pharmacology, University of California at San Francisco, 520 Parnassus Ave., San Francisco, CA 94143.

J. GEN. PHYSIOL. © The Rockefeller University Press · 0022-1295/86/09/0293/27 $1.00

Volume 88 September 1986 293–319

occurs, the ion-ion interaction helps promote a quick exit of Ca ions from the pore into the cell.

INTRODUCTION

Ca channels are highly selective (Reuter and Scholz, 1977; Lee and Tsien, 1984), yet capable of rapid rates of ion transfer (e.g., Lux and Nagy, 1981; Fenwick et al., 1982; Reuter et al., 1982; Brown et al., 1982; Cavalie et al., 1983). These properties help Ca channels to support a large influx of Ca^{2+} upon membrane depolarization and to trigger cellular functions such as contraction or secretion. The mechanism of ion permeation through Ca channels has attracted considerable interest over the past few years.

There is general agreement that the binding of Ca^{2+} to a site in the channel is an important step in its permeation (e.g., Hagiwara and Takahashi, 1967; Vereecke and Carmeliet, 1971; Hagiwara et al., 1974; Nachshen and Blaustein, 1982). However, estimates of the dissociation constant (K_d) of the site for Ca^{2+} differ by three or four orders of magnitude. On the one hand, monovalent ion flux through the Ca channel is reduced with micromolar external Ca ($[Ca]_o$), which suggests a very low value of K_d (Kostyuk et al., 1983; Hess and Tsien, 1984; Almers et al., 1984; Fukushima and Hagiwara, 1985); on the other hand, the dependence of the peak Ca current amplitude on $[Ca]_o$ points to K_d values in the millimolar range (Hagiwara, 1975; Akaike et al., 1978; Ashcroft and Stanfield, 1982; Cota and Stefani, 1984; Hess and Tsien, 1984). This discrepancy and observations of ion-ion interactions in the channel have led to the hypothesis that the Ca channel is a multi-site, single-file pore with at least two high-affinity Ca-binding sites and repulsive interactions between ions in the doubly occupied state (Hess and Tsien, 1983, 1984; Almers and McCleskey, 1984). This hypothesis owes much to previous thinking about ion permeation in gramicidin channels (e.g., Urban et al., 1980) and K channels (e.g., Hille and Schwarz, 1978).

Previous experimental work on Ca channel permeation has been carried out largely at the level of macroscopic currents. Relatively little information has been obtained with single channel current recordings in intact cells, even though they offer the possibility of determining absolute values for ion transfer rates, independently of variations in channel gating. Attempts at analysis of open Ca channel properties at the single channel level have been hampered by the brevity of opening events, rapid rundown of large conductance Ca channel activity in excised patches, and uncertainty about the cell resting potential in cell-attached patches.

Here we describe simple procedures to overcome these problems. Working with cell-attached patch recordings from freshly dissociated ventricular heart cells, we were able to measure unitary current amplitude while imposing relatively wide variations in membrane potential, ion species, and ion concentration, and to demonstrate reversal of current flow through single Ca channels. Results from single channel recordings were complemented by a systematic study of Ca channel selectivity for various divalent and monovalent ions, as determined by measurements of reversal potentials in whole cell recordings.

Preliminary reports of parts of this work have appeared in abstract form (Hess and Tsien, 1983; Tsien et al., 1983).

METHODS

Single Ventricular Myocytes and Suction Pipette Method

Single ventricular heart cells were obtained from adult guinea pig hearts by enzymatic dissociation with collagenase and hyaluronidase (see Lee and Tsien, 1984, and references therein). Whole cell recordings of Ca channel current were obtained with the suction pipette method for voltage clamp and internal dialysis as originally described by Lee et al. (1979, 1980), with some minor modifications (Lee and Tsien, 1982, 1984). After fire-polishing, pipette tips had diameters of 5–10 μm and resistances of 0.7–1.2 MΩ when filled with the internal solutions described below. In voltage-clamp experiments, ~70% of the pipette resistance was offset electronically by series resistance compensation.

The following solutions were used in the suction pipette recordings. Bath solutions contained 10 mM XCl_2, 2.8 mM $MgCl_2$ (except for the 10 mM Mg solution), 85 mM *Y*-aspartate, 146 mM sucrose, 5 mM glucose, 5 mM HEPES–TEA-OH (pH 7.4), where *X* = Ca, Sr, or Ba and *Y* = Cs, K, Na, or Li. The pipette solution (internal solution) contained 75.5 mM *Y*-aspartate, 75.5 mM *Y*-phosphate, 10 mM *Y*-EGTA, 6 mM HEPES–TEA-OH (pH 7.4). For the internal solution containing K, 10 mM TEA-Cl was added to inhibit current flow through K channels.

As a standard procedure before sucking up each cell, offset potentials in the voltage recording system were adjusted to give zero current between the pipette solution and the bathing solution (Lee and Tsien, 1984). For quantitative comparisons with other studies, all potential values should be corrected for the liquid junction potential between the pipette solution and the bath solution; measured values for the junction potential for all appropriate solution pairs were within 0.5 mV of +7 mV. As in earlier work from this laboratory (Lee and Tsien, 1984), this junction potential correction was not applied; the main focus here is on the rank order of reversal potentials, which were unaffected.

Recordings of Single Ca Channel Activity

Unitary Ca channel activity was recorded from cell-attached patches with procedures described by Hamill et al. (1981). Patch pipettes were pulled in two steps from Boralex hematocrit micropipettes (Rochester Scientific Co., Rochester NY), coated with Sylgard (Dow Corning, Midland, MI), and fire-polished. We used pipettes with tip diameters of 1–2 μm and resistances of 1.5–3 MΩ with 110 mM $BaCl_2$ in the pipette and isotonic K-aspartate in the bath. Current signals were recorded with a patch-clamp amplifier with a 10-GΩ feedback resistor in the headstage, built by V. Pantani and associates at Yale University. The signals were filtered with an eight-pole Bessel filter (−3 dB at 1 kHz), digitized at 5 kHz, and stored on a PDP 11-23 laboratory computer for later analysis. Capacitative transients were cancelled at various stages. At the time of recording, we used analog capacity compensation with three time constants. For further subtraction of capacity and leak currents at the time of analysis, current records lacking channel openings were averaged and subtracted from those records with channel activity.

Patch-clamp recordings were carried out with a bathing solution containing 140 mM K-aspartate, 10 mM K-EGTA, 10 mM HEPES-KOH (pH 7.5). Patch pipette solutions contained 10–110 mM $BaCl_2$, $CaCl_2$, or $SrCl_2$, 5 mM HEPES–TEA-OH (pH 7.5). In those solutions containing <110 mM divalent ion, TEA-Cl or sucrose was included to keep osmolarity constant.

Strategies for Accurate Determination of Unitary Current and Membrane Potential

Most of the single channel recordings were obtained in the presence of Bay K 8644 (obtained through the courtesy of Dr. A. Scriabine, Miles Institute of Preclinical Phar-

macology, New Haven, CT). This dihydropyridine Ca channel agonist greatly increases the proportion of sweeps that show long-lasting openings (Kokubun and Reuter, 1984; Ochi et al., 1984; Hess et al., 1984) and thereby facilitates accurate measurements of small unitary current. Fig. 1 shows the Bay K 8644 response in a patch containing at least three Ca channels. The first three sweeps of Fig. 1*A* illustrate the typical pattern of Ca

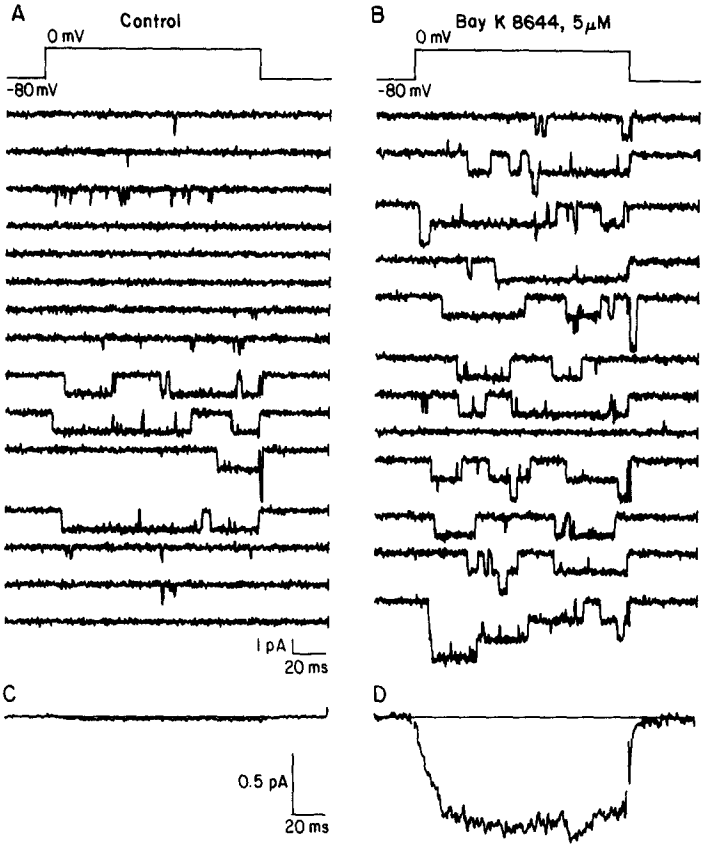

FIGURE 1. Bay K 8644 increases the proportion of sweeps with long-lasting openings. Cell-attached recordings from a patch containing at least three Ca channels. Successive current recordings were obtained at 3-s intervals before (left) and after (right) addition of 5 μM Bay K 8644 to the bath. Pipette solution: 110 mM Ba^{2+}; bath solution: isotonic K-aspartate (see text for detailed composition). Linear leak and capacity currents have been subtracted. The four sweeps with long openings in *A* were the only sweeps out of a total of 470 control records to show mode 2 activity; after exposure to Bay K 8644 (*B*), most sweeps showed long-lasting openings of at least one of the channels. (*C* and *D*) Averaged currents of all the records (470 in control, 119 after Bay K 8644). Cell 37B.

channel gating in the absence of drug. With this type of gating (called "mode 1" by Hess et al., 1984), channel openings are relatively brief (~1 ms) relative to the bandwidth limitations of the recording system, and accurate measurements of the open channel current amplitude are difficult. Every so often, however, the patch displays a very different pattern of Ca channel activity, characterized by very long channel openings ("mode 2"),

as in the cluster of four consecutive sweeps in Fig. 1*A*. The long-lasting openings make it easy to measure unitary current amplitude, but they occur relatively rarely in control runs. For example, the four clustered sweeps in Fig. 1*A* were the only sweeps out of a total of 496 that contained mode 2 activity in the absence of drug.

The proportion of sweeps with long-lasting openings was greatly increased by the addition of 5 μM Bay K 8644 to the bathing solution (Fig. 1*B*), and the average current was accordingly enhanced. In the presence of the Ca agonist, even a few sweeps gave enough long-lasting openings to allow accurate resolution of the open channel current. This made it practical to study unitary current amplitudes over a wide range of membrane potentials and permeant ion concentrations, even with unitary currents as small as 0.3 pA.

Fig. 2 presents evidence that information obtained from long-lasting openings in the presence of Bay K 8644 is generally representative of the properties of the open Ca channel. Panel *A* compares unitary current pulses in mode 1 and mode 2 sweeps in the absence of Bay K 8644 (from the same experiment as in Fig. 1*A*). While some of the short openings in mode 1 are not fully resolved, the same estimate of the unitary current amplitude (dotted lines) seems appropriate for both types of activity. Fig. 2*B* tests the possibility that the unitary current amplitude might be altered by Bay K 8644. Amplitude histograms of the mode 2 sweeps in the absence of drug (above) and in the presence of the Ca agonist (below) gave indistinguishable estimates of the unitary amplitude. The results in Fig. 2, *A* and *B*, fit nicely with our earlier findings that Bay K 8644 does not change the reversal potential of whole cell Ca channel currents (Hess et al., 1984). Like Ochi et al. (1984), we conclude that the Ca agonist does not influence the permeation mechanism. A somewhat different view was expressed by Kokubun and Reuter (1984), who reported that Ca agonists increased unitary current in neonatal rat heart cells by 4–20%. They also pointed out, however, that they could not exclude the possibility that this effect was due to a small change in membrane potential.

To eliminate uncertainties about the level of the cell membrane potential and to avoid spontaneous voltage fluctuations, all our recordings were obtained from cells bathed in a Ca-free solution containing 140 mM K-aspartate and 10 mM K-EGTA. This solution produced no visually detectable signs of cell deterioration even after incubation for >1 h. Fig. 2*C* presents evidence that this procedure was effective in zeroing the cell membrane potential. Single channel activity was recorded with 20 mM Ba in the pipette. The trace was obtained in the cell-attached mode with the isotonic K-aspartate solution bathing the cell: the elementary current was 1.07 pA. The lower trace in Fig. 2*C* was obtained with the same intrapipette potential (0 mV), immediately after excision of the patch. Despite the elimination of the cell from the recording configuration, the unitary current amplitude (i) remained unchanged, as expected if the cell membrane potential before excision had indeed been zeroed by the isotonic K solution.

Identification of L-Type Ca Channel Activity

Guinea pig ventricular cells show two distinct types of Ca channel, L-type and T-type (Nilius et al., 1985), that give rise to slowly and rapidly decaying components of whole cell Ca current in a variety of atrial and ventricular cells (Bean, 1985). Like earlier studies (e.g., Reuter et al., 1982; Cavalie et al., 1983; Hess et al., 1984), this article focuses exclusively on ion permeation through L-type Ca channels. The less common T-type Ca channels can readily be distinguished by their rapid inactivation and their relatively tiny conductance with 110 mM $BaCl_2$ as the charge carrier (~8 pS). Additional properties of T-type channel activity (Nilius et al., 1985; Nowycky et al., 1985) allowed it to be excluded from the analysis presented here. (*a*) T-type Ca channels are fully inactivated at holding potentials less negative than −50 mV. Such is the case for the whole-cell recordings

reported in this article. (*b*) Openings of T-type Ca channels appear to be bunched near the beginning of test pulses because of inactivation, not spread out throughout the depolarization as in the records in this article. (*c*) T-type Ca channels are unresponsive to 5 μM Bay K 8644.

RESULTS

Determination of Ca Channel Reversal Potential

Measurements of the reversal potential (E_{rev}) for Ca channel current provide a basic approach to evaluating the relative permeability of the channel to various

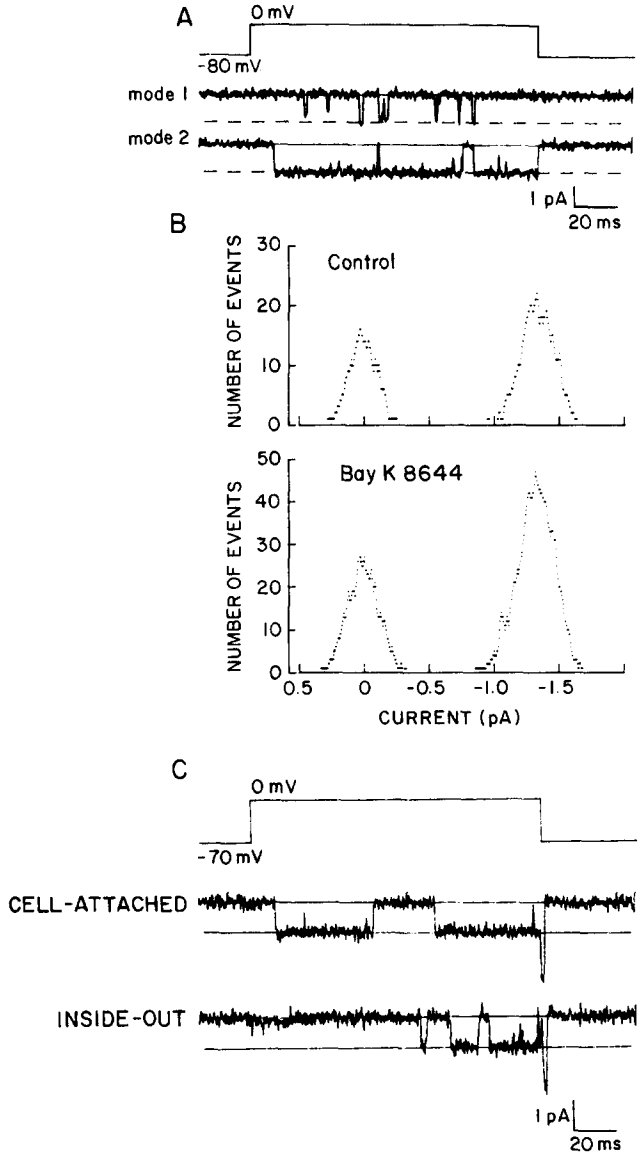

ions. E_{rev} determinations made with suction pipette recordings are particularly reliable because this method allows Ca channel currents to be isolated while the electrical potential and ionic composition on both sides of the membrane are under experimental control. Such measurements have indicated that cardiac Ca channels select strongly for divalent ions over monovalents, with Goldman permeability ratios for P_{Ca}/P_{Cs} or P_{Ca}/P_K of >1,000 (Lee and Tsien, 1982, 1984). Here we describe Ca channel currents carried by a wide range of divalent and monovalent ions and use reversal potential measurements to rank their relative permeability.

Fig. 3 shows a representative experiment where the whole cell Ca channel current was dissected by means of the organic Ca channel blocker D600. The approach is similar to that used by Lee and Tsien (1982, 1984), but the ionic species are different. In the present case, Ba^{2+} is the external charge carrier and K^+ is the internal charge carrier; we focus on these ions to facilitate comparisons between whole cell recordings and single channel *I-V* relations that will be presented later in the article (Fig. 8). Fig. 3*A* shows superimposed records of total membrane current, elicited by depolarizing pulses to test potentials ranging from −10 to +110 mV from a holding potential of −40 mV. At this relatively depolarized holding potential, Na channels and T-type Ca channels are fully inactivated, so L-type Ca channel currents are recorded without contamination. The addition of 10 μM D600 (Fig. 3*B*) eliminates net inward currents at weak depolarizations but also reduces outward currents at strong depolarizations. The current that remains after D600 is essentially linear and time independent and

---

FIGURE 2. (*opposite*) Comparison of unitary current amplitude under different experimental conditions: (*A*) mode 1 and mode 2 in the absence of drug, (*B*) mode 2 in the absence and presence of Bay K 8644, and (*C*) in cell-attached and excised patch recordings. In all three comparisons, the elementary current (*i*) remains constant. (*A*) Current records from the control run illustrated in Fig. 1, associated with a standard depolarizing voltage pulse (top trace). A mode 1 sweep with brief openings (middle trace) is compared with a mode 2 sweep with long-lasting openings (lower trace). In both cases, the dashed line indicates the value of *i* obtained from the control amplitude histogram shown in *B*. (*B*) Amplitude histograms of sweeps with long-lasting openings in the absence of drug and in the presence of Bay K 8644. The control histogram was obtained from the four sweeps in Fig. 1 that showed mode 2 activity. The histogram with Bay K 8644 was obtained by analysis of six sweeps with no simultaneous openings. Cell 37B. (*C*) External isotonic K-aspartate zeroes the membrane potential. Single channel currents were recorded with 20 mM Ba^{2+} in the pipette and ~150 mM K^+ and 5 μM Bay K 8644 in the bath (see text for exact composition). The upper trace shows the patch potential ($-V_{pip}$, where V_{pip} is the potential applied to the inside of the pipette). The middle trace shows a cell-attached patch recording. During the clamp pulse, the pipette potential was 0 mV and the transmembrane potential in the patch equals the cell resting potential. The lower trace was recorded at the same pipette potential (0 mV), 10 s after manual patch excision. The unitary amplitude was 1.07 pA both before and after excision (solid horizontal lines), which indicates that in both cases the transmembrane potential in the patch was identical. This implies that the cell resting potential before the excision was essentially zero. Cell 26K.

is presumably leakage current. Subtraction of the records in panel *B* from those in panel *A* gives the D600-sensitive current traces shown in Fig. 3*C*. The records show a well-defined reversal of Ca channel current at E_{rev} = +50 mV, where the D600-sensitive current is zero throughout the pulse. When measurements of the peak currents in Fig. 3*C* are plotted as a current-voltage relationship (Fig. 3*D*), it is evident that outward currents and inward currents increase in a nonlinear

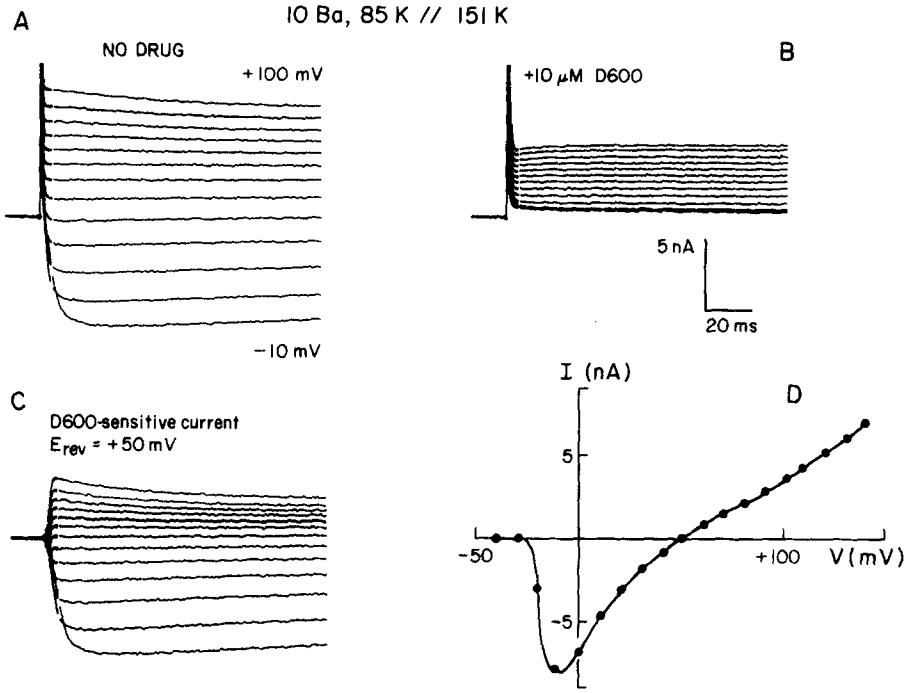

FIGURE 3. Measurement of Ca channel reversal potential from whole cell recordings. (*A*) Superimposed records of total membrane currents elicited by voltage-clamp pulses from a holding potential of −40 mV to a series of test potentials increasing in 10-mV steps from −10 to +100 mV (+7-mV correction for liquid junction potential not shown; see Methods). (*B*) Superimposed records of total membrane currents at the same potentials after the addition of 10 μM D600 to the bath. (*C*) D600-sensitive currents (difference between the currents before and after D600). (*D*) Plot of the peak of the D600-sensitive current as a function of the test potential over the full potential range explored in this cell. Bath solution: 10 mM Ba^{2+}, 85 mM K^+. Pipette solution: 151 mM K^+ (for exact composition, see Methods). Cell 186A.

fashion with the electrical driving force on either side of E_{rev} (see also Fenwick et al., 1982; Lee and Tsien, 1982, 1984).

Ca Channel Selectivity for Various Divalent and Monovalent Ions

To characterize the relative permeability of Ca channels to various divalent and monovalent cations, we carried out recordings of Ca channel current under a wide range of ionic conditions (Fig. 4). In the upper row, the extracellular

solution contained 10 mM Ca^{2+}, Sr^{2+}, Ba^{2+}, or Mg^{2+}. The extracellular and intracellular solutions contained 85 mM and 171 mM Cs^+, respectively. Cs^+ was chosen in preference to other monovalents as the main cation in order to minimize interference from K channel currents. In the families of current records

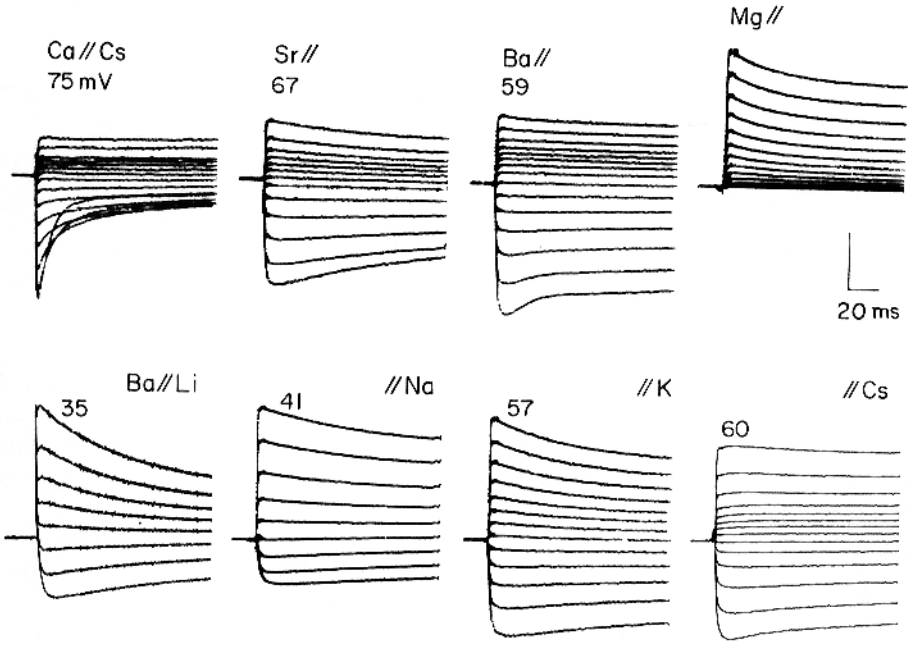

FIGURE 4. Current-voltage relations and reversal potentials with different external and internal ions. Top row (from left to right): 10 mM external Ca^{2+}, Sr^{2+}, Ba^{2+}, and Mg^{2+}, respectively; internal Cs (151 or 171 mM) throughout. Bottom row: internal Li^+, Na^+, K^+, and Cs^+ (151 or 171 mM), respectively; external Ba^{2+} (10 mM) throughout. Whole cell recordings were obtained with large suction pipettes according to the method of Lee et al. (1979) except for the lower left panel, which was obtained from a relatively small cell with a smaller gigaseal pipette (Hamill et al., 1981). The current calibration bar represents 4 pA for all panels in the top row, and 1, 6, 6, and 6 pA for the panels in the bottom row. The holding potential was −40 mV in all cases. Families of current records were obtained with test potentials spaced 10 mV apart. Test potentials spanned the following voltage ranges (mV): top row (left to right): 0–140, 10–130, 0–140, −30–120; bottom row (left to right): 10–80, 10–90, 10–140, 10–140. As in Fig. 3, all panels show current signals after subtraction of leak and capacity currents. These were determined by exposing cells to D600 (D) or verapamil (V), or by extrapolation from current signals recorded with hyperpolarizing pulses (L). Cell numbers and the method of determination of leak and capacity currents were as follows: top row (left to right): 187A (D), 199A (V), 188D (V), 191A (D); bottom row: E3G (L), 184C (L), 186B (D), 179B (L).

illustrated here, the reversal potential of the D600- or verapamil-sensitive current is most positive with extracellular Ca^{2+} and progressively less positive with Sr^{2+} and Ba^{2+}. The reversal potential was not defined with Mg^{2+} as the external divalent cation because no inward currents were ever detected with 10 mM

$[Mg]_o$ (Fig. 4, upper right) or even with 110 mM $[Mg]_o$ (records not shown). At positive potentials, the outward currents carried by Cs^+ were larger in the presence of external Mg^{2+} than with any of the other divalent cations.

The lower panels in Fig. 4 illustrate how E_{rev} varies with the species of monovalent charge carrier. The internal solution contained Li^+, Na^+, K^+, or Cs^+ at concentrations of 151 or 171 mM; the same ion was also present in the external solution at 85 mM. The main charge carrier in the external solution was 10 mM Ba^{2+}; Ba^{2+} was chosen since it is known to be much less effective than Ca^{2+} or Sr^{2+} as an activator of Ca-dependent K channels. All of the monovalent cations supported outward current through the Ca channel, but values for E_{rev} varied considerably, ranging from +35 mV with Li^+ to +60 mV for Cs^+, with intermediate values for Na^+ and K^+.

The reversal potential measurements in Fig. 4 are representative of collected data from a total of 32 cells, as illustrated in Fig. 5. Panel *A* shows results for various divalents with Cs^+ as the internal charge carrier. Judging by E_{rev}, the relative selectivity of the channel for divalent ions follows the sequence $Ca^{2+} > Sr^{2+} > Ba^{2+} \gg Mg^{2+}$. The average reversal potential with external Ca^{2+} (70.5 ± 2.36 mV, SEM) was significantly ($P < 0.05$) more positive than with external Ba^{2+} (59.2 ± 3.72 mV). The average value for external Sr^{2+} was intermediate between Ca^{2+} and Ba^{2+}; as already mentioned, all three ions were much more permeant than Mg^{2+}.

Our E_{rev} selectivity sequence for divalent cations is in good agreement with results in mouse neoplastic B lymphocytes (Fukushima and Hagiwara, 1985). Similar sequences have been reported for the ability of various current carriers to resist Co block in barnacle muscle (Hagiwara et al., 1974) and Cd block in snail neurons (Byerly et al., 1985), and for the ability of various ions to block Na currents through Ca channels in snail neurons (Kostyuk et al., 1983) and skeletal muscle (Almers et al., 1984). Matsuda (1986) showed that Mg was ~10-fold less effective than Ca in blocking cardiac Ca channel current. The sequence is one of the Eisenman sequences based on coulombic theory (see Eisenman and Horn, 1983).

According to the E_{rev} data shown in Fig. 5*B*, the relative permeability for monovalent cations follows the sequence $Li^+ > Na^+ > K^+ > Cs^+$. These results are in good agreement with E_{rev} measurements in mouse neoplastic B lymphocytes by Fukushima and Hagiwara (1985), who studied Rb but not Li. They differ somewhat from data of Kostyuk et al. (1983), who found Na > Li in snail neurons.

As Fig. 5*B* illustrates, the relative selectivity of L-type cardiac Ca channels decreases with increasing ionic diameter of group Ia cations. As in the case of the Na channel (Chandler and Meves, 1965; Hille, 1972), the selectivity sequence for these cations obeys Eisenman sequence XI, as might be expected for a high-field-strength, high-pK_a site such as a carboxyl group. The selectivity sequence is diametrically opposite to that of the acetylcholine (ACh) receptor channel (Adams et al., 1980; Lewis and Stevens, 1983), which follows the order of ionic mobility in free solution. The comparison is interesting because relatively large organic cations permeate skeletal and cardiac Ca channels in the absence of Ca (McCleskey and Almers, 1985; McCleskey et al., 1985), which suggests that Ca

channels behave in other respects as large, water-filled pores, very much like ACh receptor channels.

Monovalent Cation Selectivity in the Absence of Divalent Cation Permeation

In Fig. 5*B*, selectivity among various monovalent cations was demonstrated by showing that Ba influx is balanced by efflux of different monovalent cations at

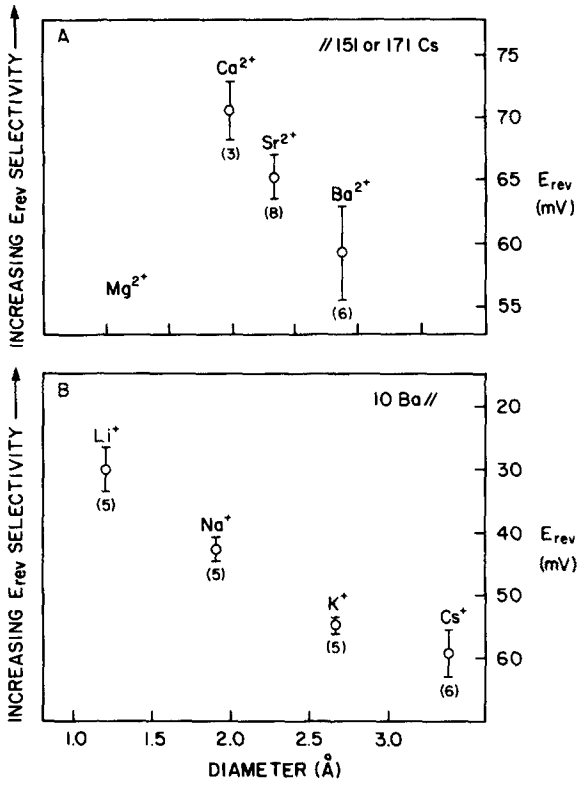

FIGURE 5. Dependence of reversal potential on the species of external divalent cation (*A*) or internal monovalent cation (*B*). Collected data from 32 cells are plotted as mean ± SEM. (*A*) E_{rev} measurements with 10 mM external divalent cation as indicated, 85 mM external Cs^+, and 151 or 171 mM internal Cs^+. (*B*) E_{rev} measurements with 10 mM external Ba^{2+}, 85 mM external monovalent cation, and 151 or 171 mM internal monovalent cation as indicated. Note that increasingly negative values of E_{rev} are plotted upward in *B* to indicate increasing selectivity to internal monovalent cations.

different values of E_{rev}. A more direct demonstration of Ca channel selectivity for monovalent ions relies on measurements of E_{rev} in the absence of permeant divalent cations, with monovalent ions as external as well as internal charge carriers. Fig. 6*A* shows whole cell currents carried by external Na^+ and internal Cs^+ in the absence of external Ca^{2+} (2 mM EGTA). To record Ca channel current with little or no contamination by other channels, Na channels were inactivated by a holding potential of −40 mV, and blocked by including tetrodotoxin in the

external solution; K channel currents were minimized by the use of Cs^+ as the charge carrier in the internal solution. As expected for Ca channel current, the remaining current was sensitive to D600 (not shown); the time course of the leak-subtracted current in Fig. 6 appears very similar to the Ca channel current carried by external Ba^{2+} in Fig. 3.

As Fig. 6*A* illustrates, the monovalent Ca channel current is inward at negative potentials (where inward Na flux outweighs the outward Cs flux), reverses between +30 and +40 mV, and is outwardly directed at more positive potentials.

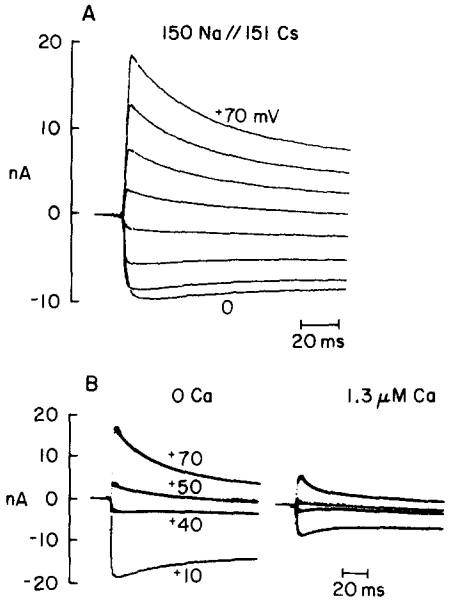

FIGURE 6. Ca channel selectivity for monovalent cations and sensitivity of monovalent currents to block by micromolar external Ca^{2+}. (*A*) Superimposed traces of net current (linear leak and capacity currents subtracted). The external solution contained 150 mM NaCl, 5 mM Na-HEPES (pH 7.4), 2 mM Na_2 EGTA, and 12.5 μM TTX. The internal solution contained 151 mM $CsCl_2$, 5 mM Cs-HEPES, and 10 mM Cs_2 EGTA. Cell 207B. (*B*) Same ionic conditions as in *A*. Net currents at four potentials in the absence (left, 2 mM Na_2 EGTA) and presence of micromolar external Ca^{2+} (EGTA replaced by 10 mM HEDTA plus 5 mM Ca^{2+}; $[Ca]^{2+}$ = 1.3 μM at pH 7.4). Cell 207G.

Reversal potential determinations with 150 mM external Na^+ and 151 mM internal Cs^+ in a total of eight cells gave E_{rev} = 40.8 ± 1.5 mV. The positive value of E_{rev} provides additional evidence that the Ca channel selects for Na^+ over Cs^+, in agreement with experiments where monovalent efflux is pitted against Ba^{2+} influx (Fig. 5*B*).

Block of Monovalent Currents through the Ca Channel by External Ca^{2+}

Fig. 6*B* provides evidence that the monovalent currents are, in fact, carried by Ca channels. The addition of 1.3 μM external Ca^{2+} reduced both inward and

outward currents without changing the reversal potential or the current kinetics. There was no clear voltage dependence of the block over the voltage range studied here (+10 to +70 mV); however, voltage dependence was seen at more negative potentials (Lansman et al., 1986).

The high sensitivity of monovalent currents to block by external Ca^{2+} was a consistent finding. The degree of inhibition illustrated in Fig. 6*B* was representative of other experiments: in three cells studied at a test potential of +10 mV, 1.3 μM Ca_o reduced the inward current carried by Na^+ to 33 ± 4% (mean ± SEM). These results support the hypothesis that the Ca channel contains a binding site with a dissociation constant of the order of 1 μM (see Introduction). The extreme sensitivity of monovalent currents to external Ca stands in contrast to other expressions of ion-channel interaction described in the section that follows.

Dependence of Elementary Current on Permeant Ion Concentration

One fundamental way to study ion-channel interactions involves measurements of ionic current as a function of the permeant ion concentration. This approach often gives information about the binding of ions to saturable sites within the pore. Taking advantage of improved methods for resolving small elementary currents at well-defined potentials, we measured unitary current amplitude, i, over a wide range of permeant ion concentrations. The direct measurement of i minimizes the need for corrections for changing surface charge, since (*a*) channel gating does not interfere with the measurement and (*b*) the permeation pathway in muscle Ca channels appears to be insulated from the surface charge of the phospholipid membrane (Coronado and Affolter, 1986). Fig. 7*A* shows examples of elementary currents recorded at 0 mV with different concentrations of Ca^{2+} or Ba^{2+} in the recording pipette. Using the Ca agonist Bay K 8644 to promote long-lasting openings, we were able to work at levels of Ca^{2+} as low as 10 mM, where the unitary current amplitude was of the order of 0.25 pA.

The mean values of i obtained from a total of 37 patches are plotted as a function of ion activity or ion concentration in Fig. 7*B*. Several points are worth noting. (*a*) At any given divalent concentration, unitary Ba current is always larger than unitary Ca current. This difference in unitary flux contrasts with channel selectivity for Ca^{2+} over Ba^{2+} judged by measurements of E_{rev}. (*b*) Values of i in 50 mM $[Ca]_o$ or $[Sr]_o$ were not significantly different (see Fig. 10*D*). (*c*) Unitary Ca and Ba currents both display a tendency to saturate with increasing permeant ion activity. Fitted saturation curves give concentration values for the apparent dissociation constant (K_d) of ~14 mM for Ca^{2+} and ~28 mM for Ba^{2+}. These values are similar to those found with macroscopic current recordings (e.g., Hagiwara, 1975; Akaike et al., 1978; Ashcroft and Stanfield, 1982; Kostyuk et al., 1983; Cota and Stefani, 1984). The estimates of K_d are at least 10^4-fold greater than the apparent dissociation constant seen with Ca block of monovalent currents.

Open Channel Current-Voltage Relations Measured with Voltage Ramps

Outward currents through cardiac Ca channels have been recorded in multicellular preparations (Reuter and Scholz, 1977; Kass and Sanguinetti, 1984), in

single cardiac cells (e.g., Lee and Tsien, 1982; Figs. 3 and 4 of this article), and in single Ca channels incorporated in planar bilayers (Rosenberg et al., 1986; see also Nelson et al., 1984; Affolter and Coronado, 1985; Ehrlich et al., 1986). We

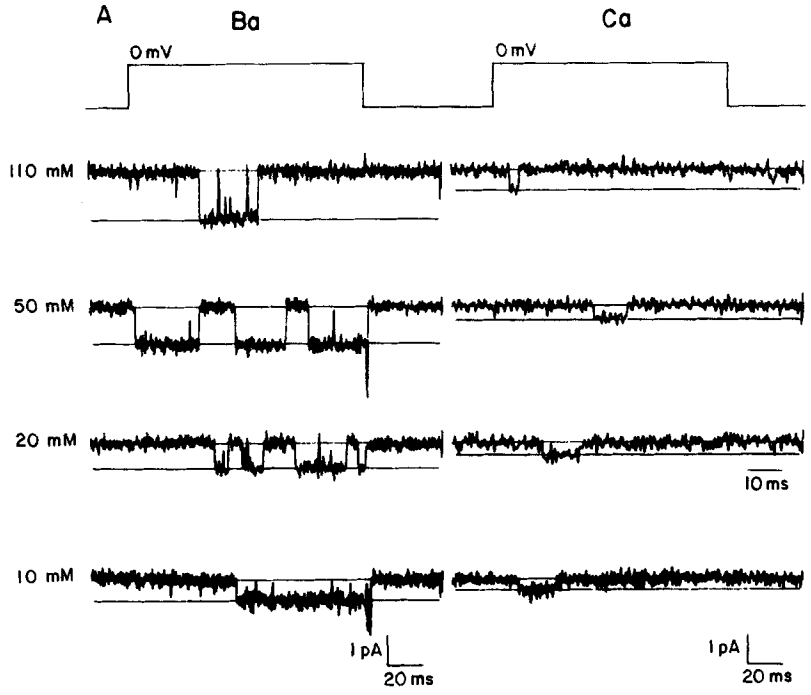

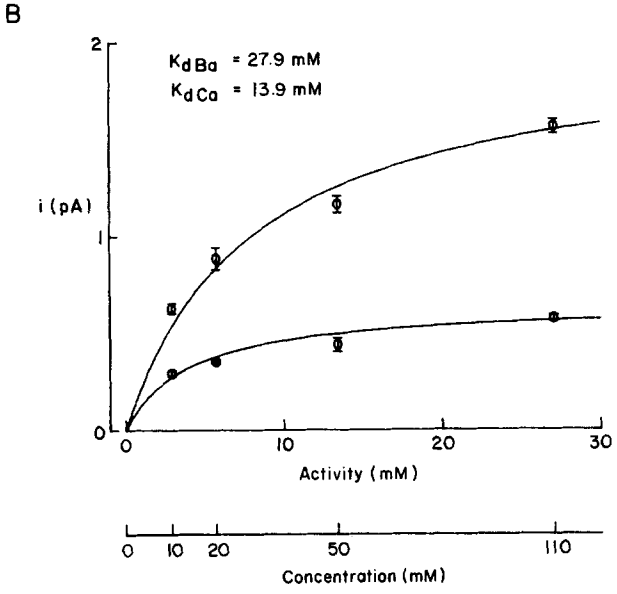

recorded open channel current-voltage curves with the hope of seeing outward unitary currents in cell-attached patches. A second objective was to gain information about how unitary fluxes of different permeant ions vary over a broad range of potentials.

The method uses ramp voltage-clamp commands (cf. Yellen, 1982), as illustrated in Fig. 8. The recordings were made with the cell-attached patch-clamp configuration and the usual procedures for zeroing the membrane potential and increasing the proportion of long-lasting channel openings. Every 4 s, the voltage command input received a ramp waveform that started from a variable potential above the holding potential and descended at a rate of 2.5 mV/ms for 100 ms (Fig. 8*A*). From the resulting current records, we selected traces that contained no detectable channel activity, and averaged them to reduce the noise. An example of the averaged null record appears as the smoother trace in Fig. 8*B*. Superimposed on this null record is an example of a current record where Ca channel activity is clearly detectable. Panel *C* illustrates the difference currents that result when the averaged null record is subtracted away from individual records. The second and fifth sweeps are examples of traces where no openings were detected. The flatness of the current records is an indication of the effectiveness of the leak subtraction procedure. The first, third, and fourth records show Ca channel openings early in the pulse and both outward and inward currents. In the sixth record, channel opening was relatively delayed and only inward current was seen.

Do the outward and inward currents arise from activity of the same kind of channel? One way of answering this question is to see whether outward currents and inward currents appear in a correlated way, as would be expected if they depend upon the availability of the same channel. This prediction was tested in the experiment illustrated in Fig. 8 by scoring for outward and inward currents on a sweep-by-sweep basis. In the vast majority of the sweeps, clearly detectable outward and inward currents occurred in the same sweep or not at all; according to chi-square analysis, the correlation was significant at the $P < 0.005$ level. This correlation would not be expected if the outward and inward currents arose from independently gated channels in the same patch.

Open channel current-voltage (*I-V*) relations were constructed from individual

---

FIGURE 7. (*opposite*) Dependence of single channel current amplitude on Ca^{2+} and Ba^{2+} concentration. (*A*) Cell-attached patch recordings. Methods as in Fig. 1 with external K-aspartate and 5 μM Bay K 8644. Every trace is from a different patch. (*B*) Elementary current at 0 mV plotted as a function of ion activity and ion concentration. Collected results from 37 patches. Activity coefficients (ionic strength in parentheses) for divalent ions in the pipette solutions of 10, 20, 50, and 110 mM concentrations: 0.294 (0.16), 0.286 (0.195), 0.269 (0.24), and 0.247 (0.33). The symbols represent mean values ± SEM. The smooth curves are best fits to the equation $i = i_{max}/(1 + K_d/[X])$, where i is the elementary current, $[X]$ is the ion activity, i_{max} is the saturating value of i at $[X]$ = infinity, and K_d is the equilibrium dissociation constant. The K_d values for Ba^{2+} and Ca^{2+} above the plot are expressed in units of concentration.

leak-subtracted current records (Fig. 8*D*). Segments of records with channel openings were first identified; a mean open current value at a particular point in the ramp was then obtained by averaging across the set of records with detectable openings. The accuracy of this method depends critically on correct leak subtraction and reasonable judgment about the occurrence of clear channel

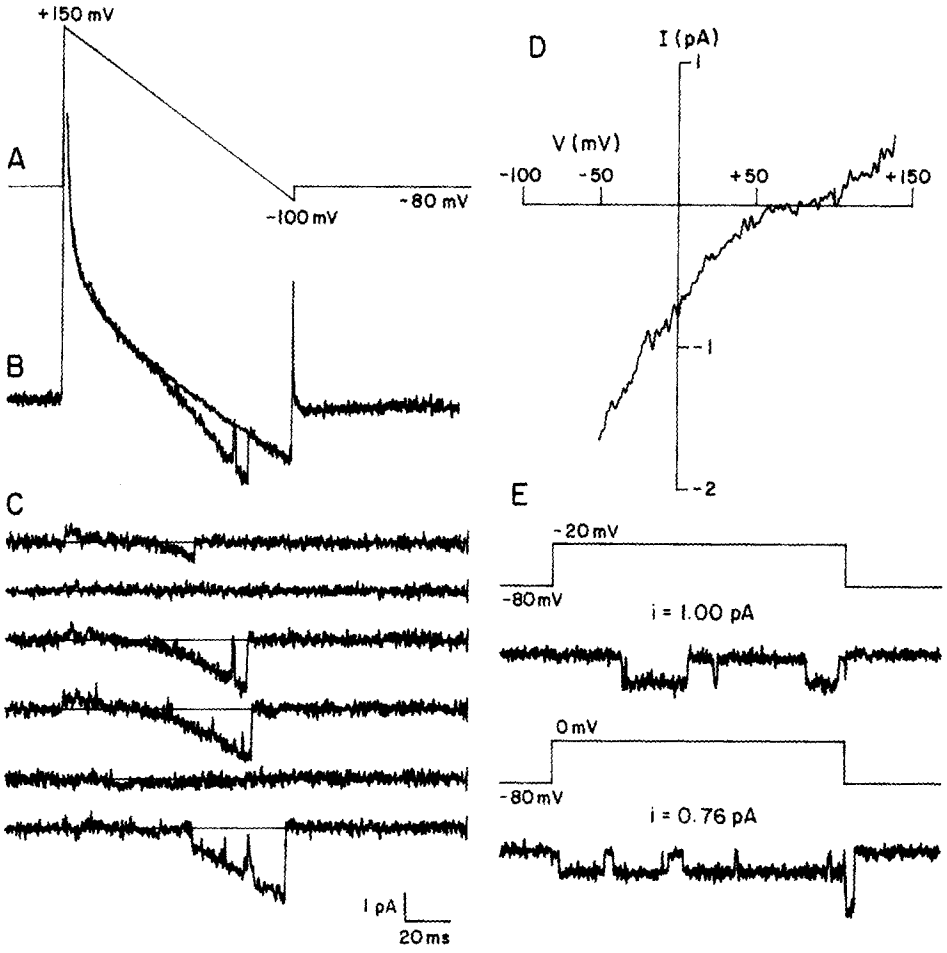

FIGURE 8. Single channel current-voltage relation obtained with voltage ramps. Cell-attached patch recordings with external K-aspartate and 5 μM Bay K 8644. The pipette contained 20 mM $BaCl_2$ and 135 mM TEA-Cl. (*A*) Voltage protocol. (*B*) Total patch currents. A sweep in which the channel opened is superimposed on the average of six sweeps with no detectable channel activity (leak trace). (*C*) A series of current records after subtraction of the averaged leak trace shown in *B*. (*D*) Open channel current-voltage relation obtained by averaging individual open channel segments identified in traces like those shown in *C*. A digital smoothing routine was used to reduce further the noise in the averaged ramp current. (*E*) Current traces obtained by steady depolarizing pulses in the same patch. The value of the elementary current measured directly at the two test potentials shown corresponds well to that obtained with the ramp protocol. Cell 25C.

activity. One test of the validity of the procedure is the excellent agreement between the values of i measured with the ramp protocol and those measured directly from elementary current pulses during normal step depolarizations in the same patch (Fig. 8*E*).

As Fig. 8*D* illustrates, this method can give open channel *I-V* relations over a wide voltage range; it is indeed possible to record outward current and reversal potentials at the single channel level. The result shown in Fig. 8 is representative of a total of six open channel *I-V* curves obtained with 20 mM Ba^{2+} in the pipette.

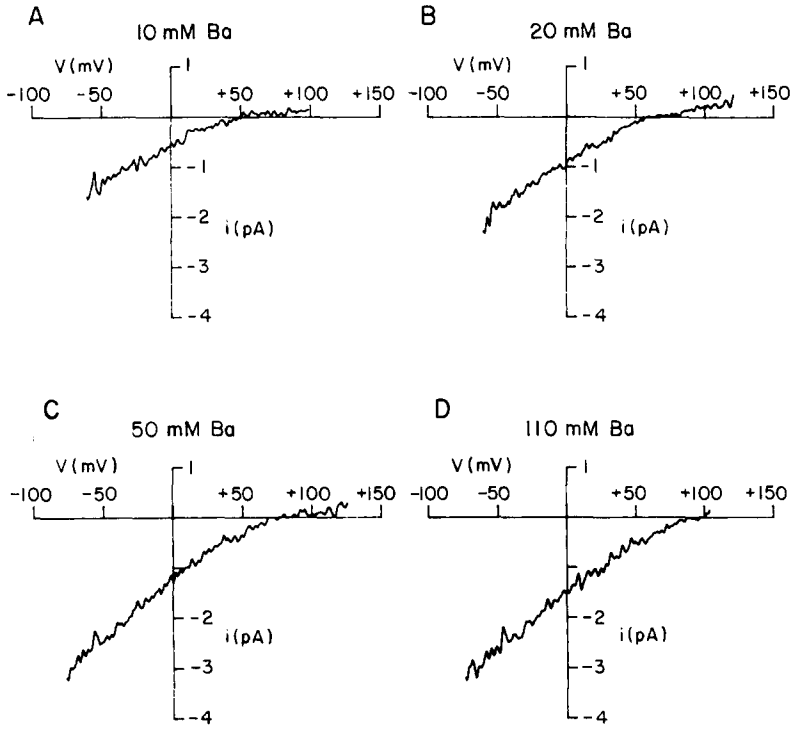

FIGURE 9. Single channel current-voltage relations with different concentrations of Ba^{2+} in the pipette. Methods as in Fig. 6. Pipette solutions: (*A*) 10 mM $BaCl_2$, 150 TEA-Cl; (*B*) 20 mM $BaCl_2$, 270 mM sucrose; (*C*) 50 mM $BaCl_2$, 90 mM TEA-Cl; (*D*) 110 mM $BaCl_2$. All solutions were buffered to pH 7.5 with 10 mM HEPES. Cells 27B, 28C, 26F, and 26E.

The main features of the *I-V* relation are: (*a*) an almost linear region at potentials up to about +30 mV (conductance, ~15 pS), (*b*) a progressive decrease of the conductance as E_{rev} is approached, (*c*) current reversal near +70 mV, and (*d*) outward current with increasing conductance (outward rectification) at potentials positive to E_{rev}.

Fig. 9 shows open channel *I-V* relations obtained with 10–110 mM Ba^{2+} in the pipette. All the *I-V*'s are close to linear in the voltage range negative to −20 mV, showing only slight downward curvature. The conductance of this linear segment

increases from 12 pS in 10 mM to 25 pS in 110 mM. The zero-current potential shifts from about +55 mV in 10 mM Ba^{2+} to about +90 mV in 110 mM Ba^{2+}.

Open channel *I-V* relations obtained with 50 mM Ba^{2+}, Sr^{2+}, or Ca^{2+} are compared in Fig. 10. The most striking difference between these three *I-V*'s is the slope conductance of the nearly linear region at negative potentials. While the conductance for Ba^{2+} is ~25 pS, that for Ca^{2+} is only ~8 pS, which is very similar to that for Sr^{2+}. The examples given for Ca^{2+} and Sr^{2+} are representative of a total of three and four patches with each ion, respectively. The mean values of the conductance below 0 mV were 7.3 pS for 50 mM Ca^{2+} and 9.5 pS for Sr^{2+}. These values are not significantly different. Because of the flatness of the *I-V*'s in the region of E_{rev}, no meaningful values for E_{rev} could be obtained with 50 mM Ca^{2+} or Sr^{2+}. We can say with confidence, however, that E_{rev} for these ions must be more positive than for Ba^{2+}.

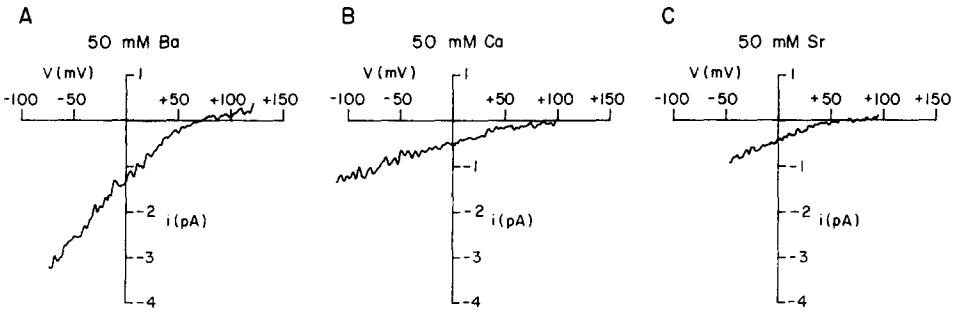

FIGURE 10. Comparison of single channel current-voltage relations with Ba^{2+}, Ca^{2+}, and Sr^{2+}. Methods as in Fig. 6. Pipette solutions as in Fig. 7*C*, with $CaCl_2$ and $SrCl_2$ substituting for $BaCl_2$ in *B* and *C*, respectively. Cells 26G, 25L, and 25S.

Current through Single Ca Channels Carried by Li^+ and Na^+

Having demonstrated outward monovalent currents through single Ca channels in cell-attached patches, in good agreement with predictions from earlier whole cell recordings, we now turn to questions about the properties of inward monovalent currents through single Ca channels. Judging by previous macroscopic current recordings (e.g., Fig. 5) and theoretical work on Ca channel permeation (Hess and Tsien, 1984; Almers and McCleskey, 1984), one would expect large unitary conductances for monovalent ions in the absence of external divalent ions.

Fig. 11 illustrates unitary Ca channel currents generated by Li or Na influx. These were recorded with 150 mM LiCl or NaCl in the patch pipette and 10 mM EDTA to make the pipette solution virtually divalent free. With either Li^+ (*A*) or Na^+ (*D*), the pattern of gating is very similar to that seen with Ba^{2+}. Sweeps with no openings (mode 0) alternate with sweeps with brief openings (mode 1) and sweeps with long-lasting openings (mode 2); Bay K 8644 greatly increased the proportion of sweeps with mode 2 gating. The kinetics of the averaged currents for both ions (Fig. 11, *B* and *E*) are also very similar to those recorded with Ba^{2+}. The main difference lies in the voltage dependence of activation: activation of Ca channels in the absence of divalent ions occurs over a potential range ~40 mV more negative than with 50–110 mM external Ba^{2+}, as might be

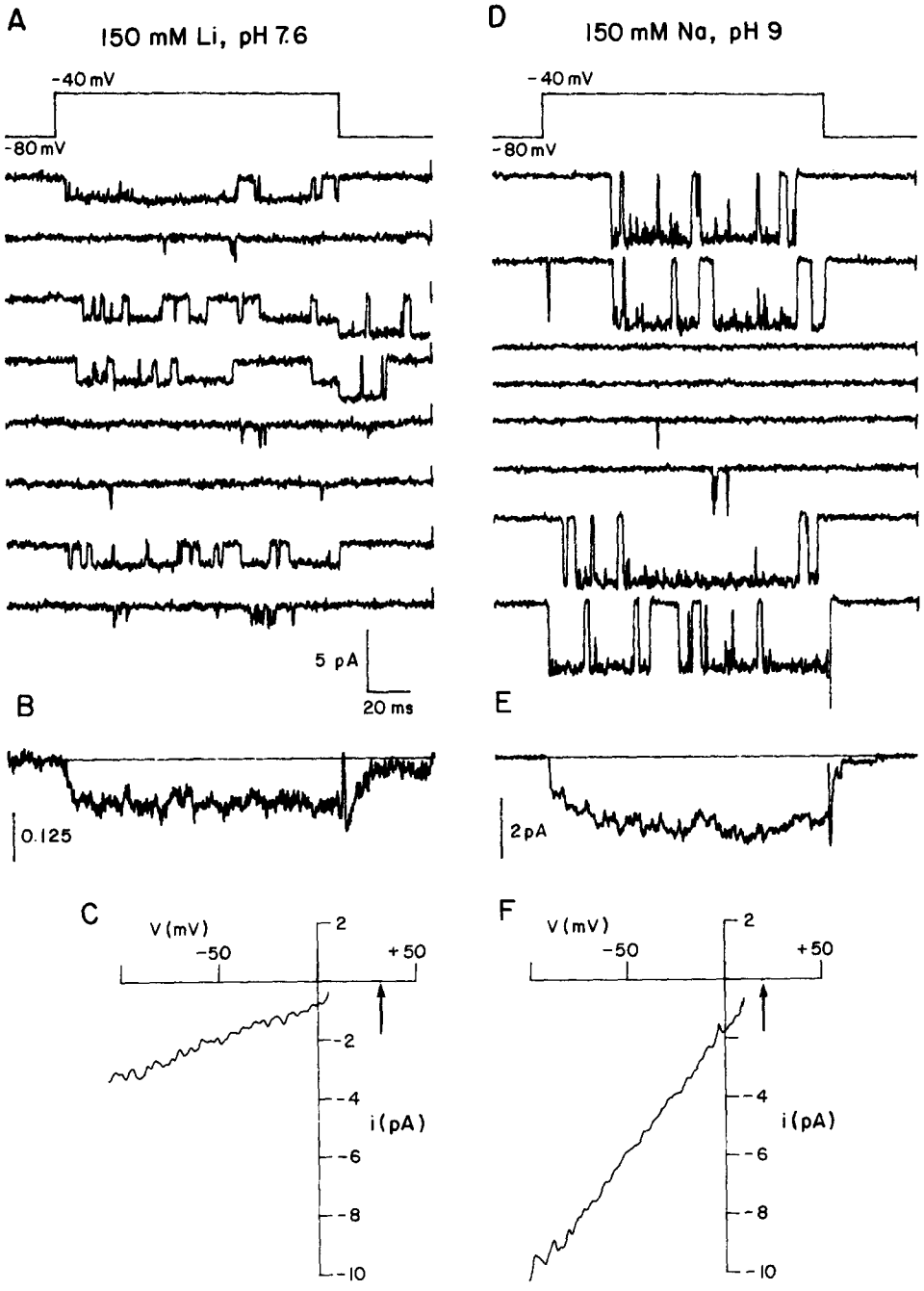

FIGURE 11. Elementary Ca channel currents carried by Li and Na ions. Cell-attached patch recordings. External K-aspartate, 10 mM $MgCl_2$, 5 μM Bay K 8644. (*A–C*) Pipette solution: 150 mM LiCl, 10 mM HEPES, 10 mM EDTA, pH 7.6. (*D–F*) Pipette solution 150 mM NaCl, 10 mM Tris, 10 mM EDTA, pH 9.0. (*A*, *D*) Current traces obtained at 3-s intervals with the voltage protocol shown on top. (*B*, *E*) Mean currents are the average of 328 and 47 successive traces in *B* and *E*, respectively. (*C* and *F*) Single channel current-voltage relations from the same patches, recorded with voltage ramps similar to those shown in Fig. 6. Cells 35R (Li^+) and 38E.

expected from the effects of changing surface potential (see Kostyuk et al., 1983).

Ramp voltage-clamp protocols produced open channel *I-V*'s (Fig. 11, *C* and *F*) that are perfectly linear over the entire voltage range studied (−100 to +20 mV). The single channel conductances are 45 and 85 pS for Li^+ and Na^+, respectively, significantly higher than those for comparable concentrations of Ca^{2+} or Ba^{2+}. With either monovalent cation, there are clearly measurable inward currents at 0 mV; selectivity of the channel for Li^+ or Na^+ over (internal) K^+ is to be expected from measurements of E_{rev} in whole cell recordings (Figs. 4 and 5). Linear extrapolation of the reversal potentials with Li^+ or Na^+ yields a value of E_{rev} that is 10–15 mV more positive for Li^+ than for Na^+. This is consistent with evidence from macroscopic reversal potential measurements (Figs. 4 and 5) that suggest that the channel selects for Li^+ over Na^+. We were unable to detect clear-cut outward unitary currents under these conditions, even though outward movements of Cs^+ were quite clear in suction pipette recordings from single cells (Fig. 6). One possible explanation is that a cytoplasmic blocker in intact cells (Ca or Mg?) obscures outward currents in cell-attached recordings, but is removed or buffered by internal dialysis in whole cell experiments.

The results with Li^+ were obtained at a pipette pH of 7.6, whereas the experiment with Na^+ was performed at pH 9. This alkaline pipette solution was necessary with Na^+ because it eliminated the partially resolved rapid blocking and unblocking transitions (most probably arising from proton block of the open channel), which made recordings of open channel *I-V*'s impossible at pH 7.6 (unpublished results). Li currents showed no sign of proton block at pH 7.6 and the amplitude of i was unchanged at pH 9.

DISCUSSION

This study was aimed at providing basic information about the mechanism of ion permeation through L-type cardiac Ca channels. The main new results include (*a*) a systematic ranking of the relative permeability to various alkali and alkaline earth cations, (*b*) a description of how unitary current varies with wide variations in membrane potential or extracellular Ca or Ba concentration, and (*c*) a demonstration of outward current through single Ca channels in cell-attached patches.

The results from single channel and whole cell recordings dovetail reasonably well in areas of overlap. The combination of approaches is particularly effective because they have different advantages and disadvantages. Whole cell recordings give much more accurate information near E_{rev}, where net current is small; they also allow manipulation of ion concentrations on both sides of the membrane with relatively little rundown (Lee and Tsien, 1984), unlike recordings of L-type Ca channel activity from excised patches (Cavalie et al., 1983; Nilius et al., 1985). On the other hand, single channel measurements eliminate the uncertainty associated with variations in channel gating, a particularly serious problem at negative potentials where channel deactivation is rapid.

The usefulness of the single channel recordings was greatly enhanced by the use of Bay K 8644 to increase the proportion of long, well-resolved openings

and isotonic K^+ to zero the resting potential; ramp voltage commands allowed information over a wide voltage range to be gathered quickly. In each case, control experiments established that the experimental maneuver did not distort the true properties of the open channel (see Figs. 1, 2, and 7). Exposure to Bay K 8644 does not alter the reversal potential determined from whole cell recordings (Hess et al., 1984), and estimates of E_{rev} from single channel data in the presence of the Ca agonist agree with E_{rev} values from whole cell recordings made in its absence.

Contrasts Between E_{rev} and i Measurements Rule Out Selectivity by Ion Rejection Alone

One of the most important aspects of this article is the comparison between information from measurements of reversal potentials and open channel fluxes. According to E_{rev} measurements (Fig. 4), Ba^{2+} is the least permeant of the divalent cations (leaving Mg^{2+} aside for the moment); Li^+ is the most permeant of the monovalents. Since $P_{Ba} \gg P_{Li}$ (Fig. 4, lower left panel), all the measurably permeant divalents come ahead of monovalents in the overall sequence of E_{rev} permeabilities. Thus, $Ca^{2+} > Sr^{2+} > Ba^{2+} \gg Li^+ > Na^+ > K^+ > Cs^+$.

The overall spread of permeabilities along the ionic series is enormous. The reversal potential of 70–75 mV with 10 mM external Ca^{2+} and 150 mM internal Cs^+ (Fig. 4, upper left panel) corresponds to a Goldman permeability ratio of ~6,000 (Lee and Tsien, 1984).

Measurements of unitary Ca channel currents with various charge carriers give significantly different selectivity sequences. Slope conductances for the measurably permeant divalents at 50 mM charge carrier rank as follows: Ba^{2+} (20 pS) > Sr^{2+} (8 pS) ~ Ca^{2+} (8 pS). This is essentially the opposite of the sequence from E_{rev} determinations. The contrast between permeability as judged by E_{rev} and i measurements holds true for at least two of the monovalents. At 150 mM charge carrier (Fig. 11), Na^+ (85 pS) > Li^+ (45 pS). Thus, for certain alkali metal cations as well as alkaline earth cations, our results are difficult to reconcile with the idea of selectivity by rejection alone. This is the prevailing interpretation for Na channels because the main difference in the energy profiles seen by permeant cations as they cross the membrane is apparent in the height of the energy barriers (Begenisich and Cahalan, 1980*a*, *b*), while binding to the two energy wells is weak for all ions. Thus, selectivity is attributed mainly to a "selectivity filter," a critical narrowing of the pore that corresponds to a barrier in the energy profile (Hille, 1984).

In the case of Ca channels, selectivity cannot take place by rejection alone; if this were true, one would expect that external cations with more positive reversal potentials would also show the largest unitary conductances, contrary to what we have observed. Our results point instead to a mechanism of selectivity involving differing ion affinities at a true binding site, corresponding to an energy well (cf. Hagiwara, 1975), such that the ion with the highest affinity (highest permeability as judged by E_{rev}) has the lowest mobility (lowest permeability as judged from the single channel conductance).

Mg ions are a notable exception to the general pattern. In this case, reversal potential and open channel flux experiments point in the same direction in suggesting that Mg^{2+} is poorly permeant. No inward Mg currents were ever detected in either whole cell or single channel recordings, even with extracellular Mg^{2+} as high as 110 mM; although E_{rev} could not be determined, it is safe to say that it could be no more positive than +10 mV with 10 mM external Mg^{2+} and 171 mM internal Cs^{+}. With respect to Mg^{2+}, cardiac Ca channels once again resemble their counterparts in neoplastic B lymphocytes (Fukushima and Hagiwara, 1985); they differ from Ca channels in frog skeletal muscle, where Almers and Palade (1981) found clear Mg currents ~1/10 as large as Ca currents. The discrepancy is probably only a matter of degree. Our own measurements of Mg block of Ba currents show relief of Mg block at negative potentials, as if Mg could enter the cell, albeit at a rate too slow to detect with current recordings (Lansman et al., 1986).

Different Measures of Ca Channel Affinity for Ca Rule Out a Single-Binding-Site Hypothesis

Fig. 7 shows that unitary Ca current increases nonlinearly with extracellular Ca activity; half-saturation occurs at ~14 mM $[Ca]_o$. The following article (Lansman et al., 1986) shows that half-block of unitary Li currents takes place at ~3 μM $[Ca]_o$. These results provide a direct demonstration at the single channel level of an $\sim 10^4$ discrepancy that has already been the focus of studies with whole cell recordings (Kostyuk et al., 1983; Hess and Tsien, 1984; Almers et al., 1984; Fukushima and Hagiwara, 1985). The single channel results remove any remaining possibility that Ca channel permeation can be accounted for by a simple one-site model, as originally proposed by Vereecke and Carmeliet (1971) and Hagiwara et al. (1974) and as elaborated more recently by others (e.g., Ashcroft and Stanfield, 1982; Cota and Stefani, 1984).

The present focus is on discriminating between two different explanations of the 4-log-unit discrepancy in half-effective Ca concentrations. The model of Hess and Tsien (1984) and Almers and McCleskey (1984) proposes that the Ca channel is a single-file pore containing at least two sites with ~1 μM K_d; the low apparent affinity of the sites for permeating Ca^{2+} is attributed to electrostatic repulsion or some other strong ion-ion interaction that opposes multiple occupancy of the pore by Ca^{2+}. On the other hand, Kostyuk et al. (1983) attribute saturation of Ca flux to a single intrapore binding site with an ~10 mM K_d, and block of monovalent currents to an external site that binds Ca^{2+} with an ~1 μM K_d. Kostyuk et al. (1983) based their model on the observation that micromolar $[Ca]_o$ reduced Na current through Ca channels in a voltage-independent manner. Their results in snail neurons are consistent with our own experiments in heart cells over a limited voltage range (Fig. 6*B*). However, at more extreme potentials, we can in fact detect voltage dependence of Ca block of monovalent currents. The single channel experiments reported in the next article (Lansman et al., 1986) show that block of Li currents by $[Ca]_o$ is relieved at strongly negative potentials. This fits nicely with the idea that the micromolar Ca blocking site is

in direct communication with the inside of the cell, and that voltage dependence expresses a direct effect of membrane field, driving Ca exit from the pore into the cell. It is difficult to explain in terms of an external regulatory site without additional ad hoc assumptions. The model of Kostyuk et al. (1983) is also difficult to reconcile with observations of ion-ion interactions within the Ca channel (Hess et al., 1983; Hess and Tsien, 1984; Almers and McCleskey, 1984; Lansman et al., 1986).

Open Channel I-V Relations

This article reports *I-V* relations for single open Ca channels over an extended voltage range, from as negative as −100 mV to as positive as +100 mV. The single channel recordings provide fresh support for the view that Ca channels can carry outward current at positive potentials (see also Rosenberg et al., 1986). As already noted, the open channel *I-V*'s show values of E_{rev} similar to those obtained in macroscopic recordings from whole cells.

Single channel recordings provide direct evidence that the upward curvature (increasing conductance) of macroscopic *I-V* relations positive to E_{rev} results from rectification at the level of single open channels rather than from an increasing degree of channel activation. According to the permeation model of Hess and Tsien (1984) and Almers and McCleskey (1984), monovalent ions can carry current only if the channel is not occupied by a divalent ion, so the outward rectification of the open channel *I-V* above E_{rev} probably reflects the voltage-dependent decrease of the channel occupancy by the external divalent cation (see also Fukushima and Hagiwara, 1985).

The properties of the open channel *I-V* in the negative voltage range are also of interest. Previous analysis of single channel recordings has shown nearly ohmic behavior at negative potentials with 50–100 mM Ba^{2+} or Ca^{2+} as charge carriers (Reuter et al., 1982; Cavalie et al., 1983). On the other hand, a decrease of the open channel conductance and saturation of i at negative potentials have been reported from estimates of i by noise analysis (Fenwick et al., 1982) and from open channel *I-V*'s obtained by analysis of tail currents (Hagiwara and Ohmori, 1982). In our direct measurements of open channel *I-V*'s, we never observed a decrease of the conductance at negative potentials at any concentration of Ba^{2+} or Ca^{2+} up to 110 mM. It seems possible that the observed decrease of the conductance in the cited studies is the result of an underestimation of i because of imperfectly resolved gating transitions (rapid tail deactivation) at negative potentials. For *I-V*'s obtained in the presence of $[Mg]_o$ (Hagiwara and Ohmori, 1982: 25 mM $[Ba]_o$ and 1 mM $[Mg]_o$), an alternative explanation is an apparent decrease of the conductance at negative potentials because of voltage-dependent block by external Mg ions (Fukushima and Hagiwara, 1985; Lansman et al., 1986).

It is remarkable that the single channel *I-V* relation is close to linear over a wide range of ionic charge carriers (Ca^{2+}, Ba^{2+}, Sr^{2+}, Li^+, and Na^+) and Ba^{2+} concentrations (10–110 mM). These observations put serious constraints on the voltage dependence of the rate-limiting step for ion transfer, whose location will

vary widely with the ionic conditions. Cell-attached patch recordings are complemented by recordings of Ca channel activity in planar bilayers (Nelson et al., 1984; Ehrlich et al., 1984, 1986; Affolter and Coronado, 1985), which allow tests of the functional symmetry of the pore under symmetrical ionic conditions (Rosenberg et al., 1986). It remains to be seen whether all of these new observations can be reconciled within the framework of Eyring rate theory descriptions of ion permeation through Ca channels.

Note added in proof: R. Levi and L. J. DeFelice (1986. *Biophysical Journal.* 50:5–9) have recently reported recordings of Na currents through single Ca channels in spontaneously beating chick heart cells. Their estimate of single channel conductance (50–90 pS) is in excellent agreement with ours (Fig. 11).

We thank R. Y. Tsien, E. W. McCleskey, R. L. Rosenberg, A. P. Fox, and J. A. Dani for helpful discussion, and S. C. Wong for technical assistance. This work was supported by grants from the U.S. Public Health Service, Miles Pharmaceuticals, and Marion Laboratories.

Original version received 17 September 1985 and accepted version received 17 March 1986.

REFERENCES

Adams, D. J., T. M. Dwyer, and B. Hille. 1980. The permeability of endplate channels to monovalent and divalent metal cations. *Journal of General Physiology.* 75:493–510.

Affolter, H., and R. Coronado. 1985. Agonists Bay-K8644 and CGP-28392 open calcium channels reconstituted from skeletal muscle transverse tubules. *Biophysical Journal.* 48:341–347.

Akaike, N., K. S. Lee, and A. M. Brown. 1978. The calcium current of *Helix* neuron. *Journal of General Physiology.* 71:509–531.

Almers, W., and E. W. McCleskey. 1984. Non-selective conductance in calcium channels in frog muscle: calcium selectivity in a single-file pore. *Journal of Physiology.* 353:585–608.

Almers, W., E. W. McCleskey, and P. T. Palade. 1984. A non-selective cation conductance in frog muscle membrane blocked by micromolar external calcium ions. *Journal of Physiology.* 353:565–583.

Almers, W., and P. T. Palade. 1981. Slow calcium and potassium currents across frog muscle membrane: measurements with a vaseline-gap technique. *Journal of Physiology.* 312:159–176.

Ashcroft, F. M., and P. R. Stanfield. 1982. Calcium and potassium currents in muscle fibres of an insect (*Carausius morosus*). *Journal of Physiology.* 323:93–115.

Bean, B. P. 1985. Two kinds of calcium channels in canine atrial cells. Differences in kinetics, selectivity and pharmacology. *Journal of General Physiology.* 86:1–30.

Begenisich, T. B., and M. D. Cahalan. 1980*a*. Sodium channel permeation in squid axons. I. Reversal potential experiments. *Journal of Physiology.* 307:217–242.

Begenich, T. B., and M. D. Cahalan. 1980*b*. Sodium channel permeation in squid axons. II. Non-independence and current voltage relations. *Journal of Physiology.* 307:243–257.

Brown, A. M., H. Camerer, D. L. Kunze, and H. D. Lux. 1982. Similarity of unitary Ca^{2+} currents in three different species. *Nature.* 299:156–158.

Byerly, L., P. B. Chase, and J. R. Stimers. 1985. Permeation and interaction of divalent cations in calcium channels of snail neurons. *Journal of General Physiology.* 85:491–518.

Cavalie, A., R. Ochi, D. Pelzer, and W. Trautwein. 1983. Elementary currents through Ca^{2+} channels in guinea pig myocytes. *Pflügers Archiv.* 398:284–297.

Chandler, W. K., and H. Meves. 1965. Voltage clamp experiments on internally perfused giant axons. *Journal of Physiology.* 180:788–820.

Coronado, R., and H. Affolter. 1986. Insulation of the conduction pathway of muscle transverse tubule calcium channels from the surface charge of bilayer phospholipid. *Biophysical Journal.* 49:197*a*. (Abstr.)

Cota, G., and E. Stefani. 1984. Saturation of calcium channels and surface charge effects in skeletal muscle fibres of the frog. *Journal of Physiology.* 351:135–154.

Ehrlich, B. E., A. Finkelstein, M. Forte, and C. Kung. 1984. Voltage-dependent calcium channels from *Paramecium* cilia incorporated into planar lipid bilayers. *Science.* 225:427–428.

Ehrlich, B. E., C. R. Schen, M. L. Garcia, and G. J. Kaczorowski. 1986. Incorporation of calcium channels from cardiac sarcolemmal membrane vesicles into planar lipid bilayers. *Proceedings of the National Academy of Sciences.* 83:193–197.

Eisenman, G., and R. Horn. 1983. Ionic selectivity revisited: the role of kinetic and equilibrium processes in ion permeation through channels. *Journal of Membrane Biology.* 76:197–225.

Fenwick, E. M., A. Marty, and E. Neher. 1982. Sodium and calcium channels in bovine chromaffin cells. *Journal of Physiology.* 331:599–635.

Fukushima, Y., and S. Hagiwara. 1985. Currents carried by monovalent cations through calcium channels in mouse neoplastic B lymphocytes. *Journal of Physiology.* 358:255–284.

Hagiwara, S. 1975. Ca-dependent action potential. *In* Membranes: A Series of Advances. G. Eisenman, editor. Marcel Dekker, New York. 3:359–381.

Hagiwara, S., J. Fukuda, and D. C. Eaton. 1974. Membrane currents carried by Ca, Sr and Ba in barnacle muscle fiber during voltage clamp. *Journal of General Physiology.* 63:564–578.

Hagiwara, S., and H. Ohmori. 1982. Studies of calcium channels in rat clonal pituitary cells with patch electrode voltage clamp. *Journal of Physiology.* 331:231–252.

Hagiwara, S., and K. Takahashi. 1967. Surface density of calcium ions and calcium spikes in the barnacle muscle fiber membrane. *Journal of General Physiology.* 50:583–601.

Hamill, O. P., A. Marty, E. Neher, B. Sakmann, and F. J. Sigworth. 1981. Improved patch-clamp techniques for high-resolution current recording from cells and cell-free membrane patches. *Pflügers Archiv.* 391:85–100.

Hess, P., J. B. Lansman, and R. W. Tsien. 1984. Different modes of Ca channel gating behaviour favoured by dihydropyridine agonists and antagonists. *Nature.* 311:538–544.

Hess, P., K. S. Lee, and R. W. Tsien. 1983. Ion-ion interactions in the calcium channel of single heart cells. *Biophysical Journal.* 41:293*a*. (Abstr.)

Hess, P., and R. W. Tsien. 1983. Calcium channel permeability to divalent and monovalent cations. A model with two ion binding sites and ion-ion interaction. *Society for Neuroscience Abstracts.* 9:509.

Hess, P., and R. W. Tsien. 1984. Mechanism of ion permeation through calcium channels. *Nature.* 309:453–456.

Hille, B. 1972. The permeability of the sodium channel to metal cations in myelinated nerve. *Journal of General Physiology.* 59:637–658.

Hille, B. 1984. Ionic Channels of Excitable Membranes. Sinauer Associates Inc., Sunderland, MA. 426 pp.

Hille, B., and W. Schwarz. 1978. Potassium channels as multi-ion, single-file pores. *Journal of General Physiology.* 72:409–442.

Kass, R. S., and M. C. Sanguinetti. 1984. Calcium channel inactivation in the calf cardiac Purkinje fiber. Evidence for voltage- and calcium-mediated mechanisms. *Journal of General Physiology.* 84:705–726.

Kokubun, S., and H. Reuter. 1984. Dihydropyridine derivatives prolong the open state of Ca channels in cultured cardiac cells. *Proceedings of the National Academy of Sciences.* 81:4824–4827.

Kostyuk, P. G., S. L. Mironov, and Ya. M. Shuba. 1983. Two ion-selecting filters in the calcium channel of the somatic membrane of mollusc neurons. *Journal of Membrane Biology.* 76:83–93.

Lansman, J. B., P. Hess, and R. W. Tsien. 1986. Blockade of current through single calcium channels by Cd^{2+}, Mg^{2+}, and Ca^{2+}. Voltage and concentration dependence of calcium entry into the pore. *Journal of General Physiology.* 88:321–347.

Lee, K. S., N. Akaike, and A. M. Brown. 1980. The suction pipette method for internal perfusion and voltage clamp of small excitable cells. *Journal of Neuroscience Methods.* 2:51–78.

Lee, K. S., and R. W. Tsien. 1982. Reversal of current through calcium channels in dialyzed single heart cells. *Nature.* 297:498–501.

Lee, K. S., and R. W. Tsien. 1984. High selectivity of calcium channels in single ventricular heart cells of the guinea pig. *Journal of Physiology.* 354:253–272.

Lee, K. S., T. A. Weeks, R. L. Kao, N. Akaike, and A. M. Brown. 1979. Sodium current in single heart muscle cells. *Nature.* 278:269–271.

Levitt, D. G. 1982. Comparison of Nernst-Planck and reaction-rate models for multiply occupied channels. *Biophysical Journal.* 37:575–587.

Lewis, C. A., and C. F. Stevens. 1983. Acetylcholine receptor channel ionic selectivity: ions experience an aqueous environment. *Proceedings of the National Academy of Sciences.* 80:6110–6113.

Lux, H. D., and K. Nagy. 1982. Single channel Ca^{2+} currents in *Helix pomatia* neurons. *Pflügers Archiv.* 391:252–254.

Matsuda, H. 1986. Sodium conductance of calcium channels of guinea pig ventricular cells induced by removal of external calcium ions. *Pflügers Archiv.* In press.

McCleskey, E. W., and W. Almers. 1985. The calcium channel in skeletal muscle is a large pore. *Proceedings of the National Academy of Sciences.* 82:7149–7153.

McCleskey, E. W., P. Hess, and R. W. Tsien. 1985. Interaction of organic cations with the cardiac Ca channel. *Journal of General Physiology.* 86:22*a*. (Abstr.)

Nachsen, D. A., and M. P. Blaustein. 1982. Influx of calcium, strontium, and barium in presynaptic nerve endings. *Journal of General Physiology.* 79:1065–1087.

Nelson, M. T., R. J. French, and B. K. Krueger. 1984. Voltage-dependent calcium channels from brain incorporated into planar lipid bilayers. *Nature.* 308:77–80.

Nilius, B., P. Hess, J. B. Lansman, and R. W. Tsien. 1985. A novel type of cardiac calcium channel in ventricular cells. *Nature.* 316:443–446.

Nowycky, M. C., A. P. Fox, and R. W. Tsien. 1985. Three types of neuronal calcium channel with different calcium agonist sensitivity. *Nature.* 316:440–443.

Ochi, R., N. Hino, and Y. Niimi. 1984. Prolongation of calcium channel open time by the dihydropyridine derivative Bay K 8644 in cardiac myocytes. *Proceedings of the Japan Academy Series B Physical and Biological Sciences.* 60:153–156.

Reuter, H., and H. Scholz. 1977. A study of the ion selectivity and kinetic properties of calcium dependent slow inward current in mammalian cardiac muscle. *Journal of Physiology.* 264:17–47.

Reuter, H., C. F. Stevens, R. W. Tsien, and G. Yellen. 1982. Properties of single calcium channels in cardiac cell cuture. *Nature.* 297:501–504.

Rosenberg, R. L., P. Hess, J. Reeves, H. Smilowitz, and R. W. Tsien. 1986. Calcium channels in planar lipid bilayers: new insights into the mechanisms of permeation and gating. *Science.* In press.

Tsien, R. W., B. P. Bean, P. Hess, and M. Nowycky. 1983. Calcium channels: mechanism of beta-adrenergic modulation and ion permeation. *Cold Spring Harbor Symposia on Quantitative Biology.* 48:201–212.

Urban, B. W., S. B. Hladky, and D. A. Haydon. 1980. Ion movements in gramicidin pores: an example of single-file transport. *Biochemica et Biophysica Acta.* 602:331–354.

Vereecke, J., and E. Carmeliet. 1971. Sr action potentials in cardiac Purkyne fibres. II. Dependence of the Sr conductance on the external Sr concentration and Sr-Ca antagonism. *Pflügers Archiv.* 322:73–82.

Yellen, G. 1982. Single Ca^{++}-activated nonselective cation channels in neuroblastoma. *Nature.* 296:357–359.